Radboud University Nijmegen

Faculty of Science

Two-dimensional Quantum Gravity coupled to a scalar field

Obtaining a statistical distribution of the labels of colorful quadrangulations using gasket decomposition

Thesis BSc Physics and Astronomy

Author:
Pim Kelderman

Supervisor:
dr. Timothy Budd

Second reader:
dr. Frank Saueressig

March 2024

Contents

1 Introduction

1.1 Motivation

Over recent decades, physicists have been trying to unify the fundamental laws of Einstein's theory of General Relativity and Quantum Mechanics. The search for such a theory of *Quantum Gravity* has, therefore, become a well-studied open problem with many different approaches. The problem lies explicitly in creating a theory of gravity that is consistent with both General Relativity and Quantum Mechanics.
On the one hand, we have Quantum Mechanics, which describes the behavior of nature on the smallest of scales, ranging from atomic nuclei down to the Planck scale. Its framework describes three of the four fundamental forces of physics: the electromagnetic force, the weak force, and the strong force. In Quantum Mechanics, quantities such as energy and momentum are quantized. Furthermore, particles are described by a wave function that, when squared, gives a probability distribution of the position of the particle. Quantum Mechanics is often formulated via the Feynmann path integral formalism,

$$Z = \int \mathcal{D}\mathbf{x}\, e^{iS[\mathbf{x}]/\hbar}. \tag{1.1}$$

Here, one computes an infinite-dimensional integral over all possible paths $\mathbf{x}$ a particle can take from point A to B, where each path contributes with a phase based on its action [1]. Performing a Wick rotation, we go to the Euclidean path integral formalism,

$$Z = \int \mathcal{D}\mathbf{x}\, e^{-\tilde{S}[\mathbf{x}]/\hbar}. \tag{1.2}$$

This now provides a probability distribution of the path a particle might take, which is, therefore, non-deterministic, or *random*.

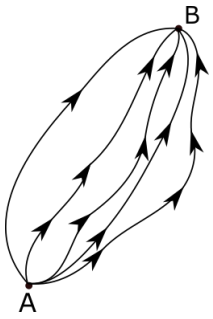

Figure 1.1: A few of the infinitely many possible paths between points A and B in the path-integral formalism. Source: Wikipedia (Path integral formulation).

On the other hand, we have General Relativity, which describes the fourth and final fundamental force: gravity. It explains how nature works on a cosmic scale, from planets and stars to the entire universe. General Relativity is a *geometric* theory that states that we live in a 4-dimensional universe consisting of three space dimensions and one time dimension, which are coupled to form a 4D spacetime. The energy density content of this spacetime determines its curvature, which in turn governs the motion of matter and radiation [2]. John Wheeler famously put this as, *"Spacetime tells matter how to move; matter tells spacetime how to curve."*[3] Gravity is essentially a manifestation of the *geometry* of the underlying spacetime.
However, why even bother trying to merge these theories when they both do a fantastic job of describing the world in their relative regimes? In our everyday lives, we do not

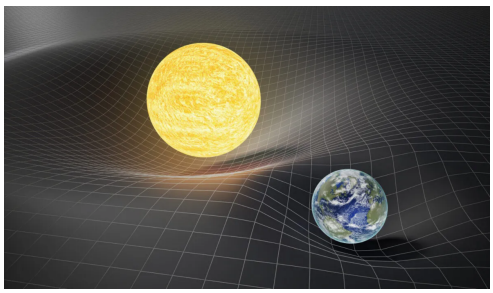

Figure 1.2: A visualization of spacetime curved by the sun and by the earth from General Relativity. Source: SciTechDaily

encounter situations where there is a need for a Quantum Gravity theory. However, there are objects and situations where the two scales meet. Two examples of this are black holes and the Big Bang. Let us take a typical black hole as an example. Inside, there is an infinitely small singularity with a mass usually greater than the mass of our sun. Hence, the quantum regime meets the realms of General Relativity. To understand these mysterious objects, one would need a theory of Quantum Gravity, as the current description of physics breaks down beyond the event horizon [4]. Therefore, a theory of Quantum Gravity can offer numerous novel or groundbreaking perspectives and understandings.

1.2 Euclidean Quantum Gravity

One attempt at such a theory is Euclidean Quantum Gravity. Here, we take the path integral formalism from quantum mechanics (1.1), but we now integrate over all possible geometries [5, p.68-73],

$$Z = \int \mathcal{D}g\, e^{iS_{EH}[g]/\hbar}. \tag{1.3}$$

In particular, this integral is taken over all possible geometries g on a d-dimensional spacetime manifold M. In this integral, every geometry carries an appropriate weight, i.e., the Euclidean Einstein-Hilbert action

$$S_{\mathrm{EH}}[g] = \frac{1}{16\pi G}\int_M \mathrm{d}^d x\sqrt{g}(-R + 2\Lambda). \tag{1.4}$$

By now performing a formal Wick rotation on the path integral (1.3), it becomes a partition function, with which we arrive at the starting point of Euclidean Quantum gravity,

$$Z = \int \mathcal{D}g\, e^{-S_{EH}[g]}. \tag{1.5}$$

One of the significant advantages of Euclidean quantum gravity over the Feynman path integral of Lorentzian quantum gravity is that the integrand is real and positive, which allows for a statistical interpretation of the partition function Z. In this interpretation, the term $e^{-S_{\mathrm{EH}}[g]}$ plays the role of the Boltzmann weight assigned to the geometries. This statistical interpretation enables us to view the system as a statistical ensemble, where the geometries are the different configurations of the ensemble, and the weight assigned to each geometry is proportional to its probability of occurrence in the ensemble, turning this problem into a statistical problem. However, finding a probability measure

$$\frac{1}{Z}\mathcal{D}g\, e^{-S_{EH}[g]} \tag{1.6}$$

proves itself quite a challenge. For example, one of the problems we encounter is that the Einstein-Hilbert action is unbounded from below for dimensions higher than two. This implies that highly curved geometries will receive much higher Boltzmann weight than the classical Einstein solutions, known as the *conformal factor problem*. I refer the reader to [6, p. 2-4] for an overview of this and other issues and reported progress.
For 2D, however, the Einstein-Hilbert action is invariant of the topology. So, we can fix the 2D manifold to be the 2-sphere S^2, so that only the volume $V = \int_{S^2} \sqrt{g}$ depends on the metric [6]. Hence, every geometry of volume V now receives an equal Boltzmann weight. Therefore, the probability measure of this integration over V should be equivalent to sampling a metric on S^2 uniformly at random. However, we are still left with an infinite dimensional integral over all Riemannian geometries on S^2. As a starting point, we can restrict ourselves to only looking at piecewise flat geometries, which brings us to the study of Random Geometry.
Despite the 2D case being a simpler model compared to realistic 4D spacetimes, it is by no means trivial. It can serve as an interesting test bed for our mathematical methods, from which we can learn valuable lessons.

1.2.1 Random geometry

As stated in the previous section, we want to look at discrete geometries. Random geometry serves as the mathematical description for these discrete geometries, and in this section, we will conceptually see what Random geometry entails.
Specifically, we look at geometries made from n identical building blocks. If we increase the number of building blocks to infinity and shrink their size, we will obtain a good approximation of the continuous case. The major advantage of using discrete models is that their properties are much easier to analyze. We may find interesting relations and study their asymptotic behavior in the large n limit. The building blocks are Euclidean polygons glued together to form a random geometry.

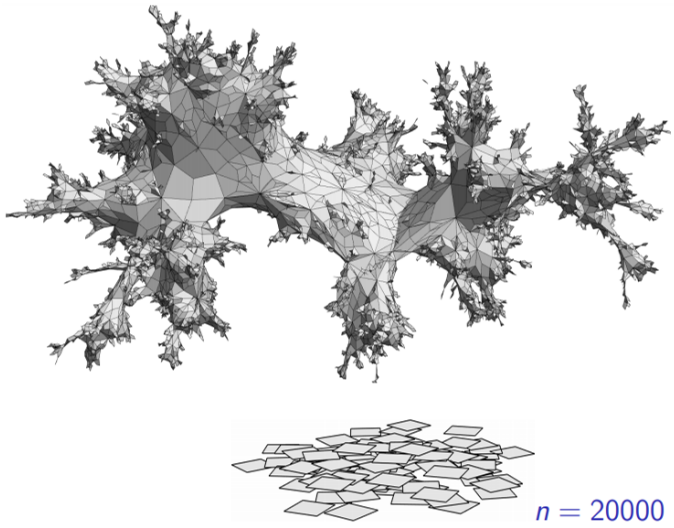

Figure 1.3: A faithful attempt of a 3D embedding of a 2D random geometry, which is obtained by gluing together $n = 20000$ Euclidean quadrangles. Image credit: dr. Timothy Budd.

Which polygons you take does not matter, as in the limit $n \to \infty$ the geometries all belong to the same *universality class* [7]. In this thesis, we will stick to quadrangles

as our building blocks because, with some induced conditions, they offer a convenient combinatorial model, as will be seen later. We call these geometries obtained b the gluing of Euclidean quadrangles *quadrangulations*.

1.2.2 Universality classes and Liouville Quantum Gravity

The random geometry in Figure 1.3 is made out of Euclidean quadrangles, but changing this to any other p-gon does not change the geometry, as stated earlier. This implies that these two models are in the same *universality class*. If by changing any microscopic details of a model the macroscopic structure of the surface is changed, we say these are in a different universality class. Fractal characteristics are represented by *critical exponents*. I refer the reader to [8] for a deeper analysis of universality classes and critical exponents. For us, it is only interesting to know in what universality class we are. Therefore, we link this to *Liouville Quantum Gravity* (LQG), whose content goes beyond the scope of this thesis. However, parameter values might be interesting to know. In the case of absence of matter, we have matter central charge $\mathbf{c} = 0$, and LQG universality class parameter $\gamma = \sqrt{8/3}$, which is called *pure gravity*. By adding a massless scalar field, we add 1 to the matter central charge, such that it becomes $\mathbf{c} = 1$, which corresponds to $\gamma = 2$, a critical value in LQG [9].

1.2.3 Adding matter

Until now, we have considered Euclidean Quantum Gravity in the absence of matter. A natural and interesting question to ask now is what happens when we add matter to the problem. The added matter should alter the geometry of the spacetime, which consequently determines the dynamics of the matter. Therefore, one might ask what kind of influence matter has on each other. This is equivalent to asking whether there is some kind of correlation between the matter and what this correlation looks like. To do this, we will couple our 2D Euclidean quantum gravity to a massless scalar field, which we know to describe spin-0 particles in Quantum Field Theory [10]. Such a scalar field ϕ would take a scalar value on every point of our 2D geometry. The partition function then becomes

$$Z = \int \mathcal{D}g\mathcal{D}\phi \; e^{-S[g,\phi]}, \tag{1.7}$$

where the weight is now dependent on both the metric and the scalar field,

$$S[g,\phi] = S_{\mathrm{EH}}[g] + \int d^2x\sqrt{g}\partial_\mu\phi\partial^\mu, \tag{1.8}$$

and where we integrate now over all possible metrics g and all possible scalar fields ϕ of a manifold [8].

1.3 Goal and Outline

This thesis will explore 2D Euclidean quantum gravity coupled to a scalar field. In particular, we aim to find a probability distribution and a scaling limit of the values of a scalar field on random geometries and thereby deduce quantum gravitational effects on the scalar field theory.
To this end, we will introduce the theory of Random Geometry by defining planar maps and disks and how to enumerate these objects in Section 2. In Section 3, we continue by coupling a scalar field to the context of planar maps, which is done via integer labeling of the vertices of these maps. Subsequently, we introduce a specific model, which we then analyze. In Section 4, we additionally mark one of the vertices of our map, set up a recurrence relation, and work our way toward the desired probability distribution and scaling limit of the values of the scalar field.

2 Planar maps, disks and their enumeration

As a start, it is useful to get acquainted with the mathematical theory that lays the foundation of this thesis. Therefore, we will introduce the mathematical objects and machinery we need later. There is a lot of information available on the theory, and many books have been written that go way beyond the scope of this thesis. Therefore, we will stick only to the most important aspects necessary for understanding the topic at hand and make only small excursions for interesting and noteworthy points. This section is largely based on the work of Budd [6].

2.1 Planar Maps

In this section, we will start by introducing graphs, how they embed on surfaces, and briefly mention Euler's theorem. Then, we work our way towards a definition for planar maps and disks and mention some specified versions of them.

Definition 2.1. A *multigraph* G is a finite set of *vertices*, *edges* and an *incidence map* $(V(G), E(G), \mathcal{I})$, where sets of vertices and edges are respectively $V(G)$ and $E(G)$. The incidence map $\mathcal{I} : E(G) \to V(G) \times V(G)$ connects two vertices by an edge. These vertices are then referred to as the *endpoints* of said edge.

In this definition, we allow for *loops*, which are edges whose endpoints are the same vertex, and *multiple edges*, which means that more than one edge may connect the same two vertices. We call a graph *simple* if it does not contain loops or multiple edges. It is also possible to have vertices that are not connected by any edge. Therefore, we define connected multigraphs.

Definition 2.2. A *connected multigraph* is a multigraph where every pair of vertices is connected by at least one edge. In other words, starting from any vertex and tracing along the edges, it is possible to reach any other vertex in the graph.

The *degree* of a vertex is the number of edges incident to it. See Figure 2.1 for an example of a connected multigraph.

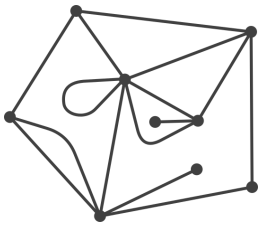

Figure 2.1: An example of a multigraph, which has one loop and two multiple edges. The degree of the top right vertex is four, the degree of the bottom right face is seven, and the degree of the outer face is five.

Now let us work our way from graphs to maps, and in particular planar maps.

Definition 2.3. A *closed oriented surface* S is an oriented, compact, and connected two-dimensional manifold with no boundary. The *genus* g of the surface is the number of holes it has. A closed surface of genus g is *homeomorphic* to a sphere with g handles attached.

On these surfaces, we want to properly embed our graphs.

Definition 2.4. A proper *embedding* of a connected multigraph G into a surface S is a drawing of G on S such that:

- Each vertex of G is represented by a unique point in S;
- Each edge in G is represented in S by a non-self-intersecting (curved) line segment homeomorphic to $[0, 1]$. No two edges intersect, apart from where they meet at the vertices;
- The edges enclose a collection of topological disks ($S \setminus G$), which are the faces of the graph.

Definition 2.5. A *planar map* $\mathfrak{m}$ is a connected multigraph embedded in a genus zero surface.

Figure 2.2: A connected multigraph properly embedded on S^2. Source: Timothy Budd.

To add a bit of generality here, a *genus-g map* is a connected multigraph embedded in a surface of genus g. In a genus-g map, the number of vertices, edges, and faces are related. This simple yet interesting relation is given by Euler's theorem.

Theorem 2.6 (Euler's theorem)**.** *For a map $\mathfrak{m}$, the sets of vertices, faces, and edges are respectively denoted by $V(\mathfrak{m})$, $F(\mathfrak{m})$ and $E(\mathfrak{m})$. Euler's theorem relates the number of vertices, faces and edges in the following way,*

$$|V(\mathfrak{m})| + |F(\mathfrak{m})| - |E(\mathfrak{m})| = 2 - 2g. \tag{2.1}$$

Here, $F(\mathfrak{m})$ is the set of *faces*. In Figure 2.2, for example, the faces are the blue areas enclosed by a set of edges. Note that the space outside a map (such as in Figure 2.3) also represents a face, called the *outer face*. The *degree* of a face is the number of edges that form its boundary[1]. Since we will only deal with planar maps in this thesis, we will stick to $g = 0$ from now on. We can see that these planar maps describe discrete surfaces when we think of the faces as regular unit polygons that are glued together. Describing discrete surfaces via the gluing of regular Euclidean unit polygons is done in [6]. It provides an intuitive way to visualize the discrete surfaces, yielding a redundant description, however. We are, of course, interested in a precise way to enumerate discrete surfaces. Just planar maps are not enough for this pursuit. Because, say, there exists a permutation that non-trivially permutes the vertices and edges of a map but yields the same map (an orientation-preserving homeomorphism of the sphere). These are called *automorphisms*. Multiple embedded graphs then correspond to the same planar map $\mathfrak{m}$. To solve this, we add a direction to one of the edges of the map. We call these rooted planar maps (see Figure 2.3), which now provide an unambiguous combinatorial representation of discrete surfaces. Now that this is out of the way, we will define some specified versions of planar maps.

[1] Every edge can therefore be seen to contribute twice to a face degree. Once for one face and once for the face on the opposite side of the edge.

Definition 2.7. An *even map* is a map whose faces are all of even degree. Even planar maps are *bipartite maps*, which have the property that you can color all vertices with two colors and have no neighboring vertices share the same color.[2]

We now arrive at the definition of quadrangulations, which will be studied in this thesis.

Definition 2.8. A *quadrangulation* is a planar map whose faces are all of degree 4.

We will need some additional specifications to extract the desired probability distribution, but these will be introduced later.

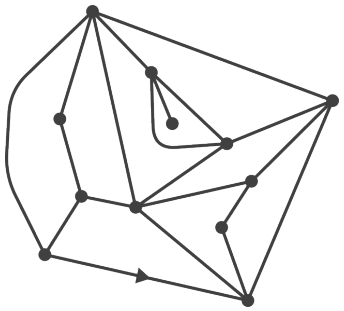

Figure 2.3: An example of a rooted quadrangulation.

In particular, we will work with quadrangulations on a disk. To conclude this section, let us define what a disk is.

Definition 2.9. A *disk* is a planar map with a boundary. So now, it is embedded in an *open surface*, which is a surface that is homeomorphic to a topological disk and, as such, has a boundary. The outer face of the map can have arbitrary degree, and the map's boundary represents the boundary of the surface it is embedded on.

Remark. Euler's theorem becomes now $|V(\mathfrak{m})| + |F(\mathfrak{m})| - |E(\mathfrak{m})| = 2 - 2g - b$, where b is the number of boundaries. Disks have one boundary and genus zero, like spheres. For quadrangulations on a disk, this becomes $|V(\mathfrak{m})| + |F(\mathfrak{m})| - |E(\mathfrak{m})| = 1$

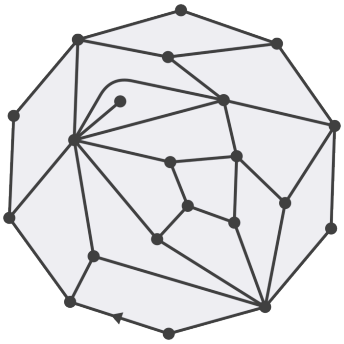

Figure 2.4: A quadrangulated rooted disk. The faces have a light tone to emphasize that the outer face is excluded and that it thus is a disk.

[2]Even maps of genus $g > 0$ do not necessarily exhibit this property.

2.2 Generating functions

We will now introduce generating functions, which will prove very useful or even essential for working with planar maps. Generating functions essentially convert the counting problem of some combinatorial object into an algebraic problem, which has the advantage that we can manipulate them. How we exactly convert our problem to a counting problem will be seen later in Section 2.3. Let us begin by defining generating functions.

Definition 2.10. A *generating function* of a sequence of numbers $(a_n)_{n\geq 0}$ is a *formal* power series $\sum_{n=0}^{\infty} a_n x^n$, that takes the elements of the sequence as its coefficients.

It is a formal power series, as more often than not, these diverge, still allowing us to work with them. The radius of convergence $\rho \in \mathbb{R}$ are the values x can take and converge. Thus, for $|x| < \rho$, the sum converges and does so to its analytical form. A simple example is the geometric series, where we have $a_n = 1$, $\forall n \geq 0$, such that

$$\sum_{n=0}^{\infty} x^n = \frac{1}{1-x}. \tag{2.2}$$

This holds for all $|x| < 1$, so $\rho = 1$, and the analytic form is $F(x) = \frac{1}{1-x}$. Therefore, we can work with these analytical forms to analyze sequences. To extract the coefficient of x^n of F(x), we use the notation $a_n = [x^n]F(x)$. An obvious extension to this is $[x^n](x^m F(x)) = [x^{n-m}]F(x) = a_{n-m}$. Generating functions can also be used to solve recurrence relations. For example, we can take the sequence defined by $a_k = 2a_{k-1}$, with $a_0 = 3$. Its generating function is given by

$$F(x) = \sum_{n=0}^{\infty} a_n x^n = a_0 + \sum_{n=1}^{\infty} a_n x^n = 3 + \sum_{n=1}^{\infty} 2a_{n-1}x^n \tag{2.3}$$

$$= 3 + 2x \sum_{n=1}^{\infty} a_{n-1}x^{n-1} = 3 + 2xF(x). \tag{2.4}$$

Hence, $F(x) = \frac{3}{1-2x}$. Thus, generating functions provide a means to algebraically work with these sequences and apply all operations that apply to power series and functions if they converge. The combinatorial objects we work with in this thesis are maps, so we will now see how generating functions are applied to the context of planar maps and, in particular, disks.

2.3 Partition function for maps

Before we set the general generating function for rooted planar maps, we need a few ingredients. Firstly, we denote the space of all rooted planar maps by $\mathcal{M}$, over which we will take the summation. For every map $\mathfrak{m} \in \mathcal{M}$, we assign a weight t for every vertex. Lastly, we want to assign a weight q to every face of the map. Let us, therefore, define the weight sequence $\mathbf{q}$.

Definition 2.11. The weight sequence $\mathbf{q} = (q_1, q_2, \dots)$ provides a weight for the faces of a map $\mathfrak{m}$. So, q_k is the weight assigned to every face of $\mathfrak{m}$ of degree k.

Therefore, we now consider the following generating function for the partition function,

$$Z(t, \mathbf{q}) = \sum_{\mathfrak{m}\in\mathcal{M}} t^{|V(\mathfrak{m})|} \prod_{f\in F(\mathfrak{m})} q_{\deg(f)}. \tag{2.5}$$

To get a bit of a feeling for this, let us look at Figure 2.1 (and assume for a second it is rooted). This map contributes to the partition function by a term $t^9 q_1 q_2 q_3^2 q_4 q_5^2 q_7$.

Definition 2.12. If $Z(t, \mathbf{q})$ is finite, we can normalize the sum by $1/Z(t, \mathbf{q})$. This gives us a probability distribution on $\mathcal{M}$, which we call the $(t, \mathbf{q})-$*Boltzmann planar map.*

To specify this, we will be looking at disks. For planar maps, the outer face is also a face that needs to be considered. For disks, we exclude this outer face or *root face* f_r, which is the face that lies on the left side of the root edge. The generating function for these disks with controlled boundary length ℓ is thus given by

$$W^{(\ell)}(t, \mathbf{q}) = \sum_{\substack{\mathfrak{m} \in \mathcal{M} \text{ with} \\ \deg(f_r) = \ell}} t^{|V(\mathfrak{m})|} \prod_{f \in F(\mathfrak{m}) \setminus \{f_r\}} q_{\deg(f)}. \tag{2.6}$$

Here, we set $W^{(0)}(t, \mathbf{q}) = t$ by convention, taking into account the map that only consists of one vertex and no edges.

2.3.1 Criticality

When using formal power series to compute the partition function, we disregarded convergence issues. However, we eventually want to look at the statistical properties of random planar maps. Therefore, we have to ensure that probability measures are sensible. Therefore, $\mathbf{q}$ is admissible if $Z(t = 1, \mathbf{q}) < \infty$ or $W^{(\ell)}(\mathbf{q}) < \infty$. For generating functions, we had a radius of convergence ρ. If a generating function converges for $x = \rho$, but not for $x > \rho$, we call ρ the *critical value.*

2.4 Tutte's loop equation

We can obtain an equation for the generating function for disks of controlled boundary length ℓ_1. To this end, we can see that for $\ell \geq 1$, we can make a decomposition by removing the root edge, and construct an equation for this. By removing the root edge, we either have two maps or a map with one face less.

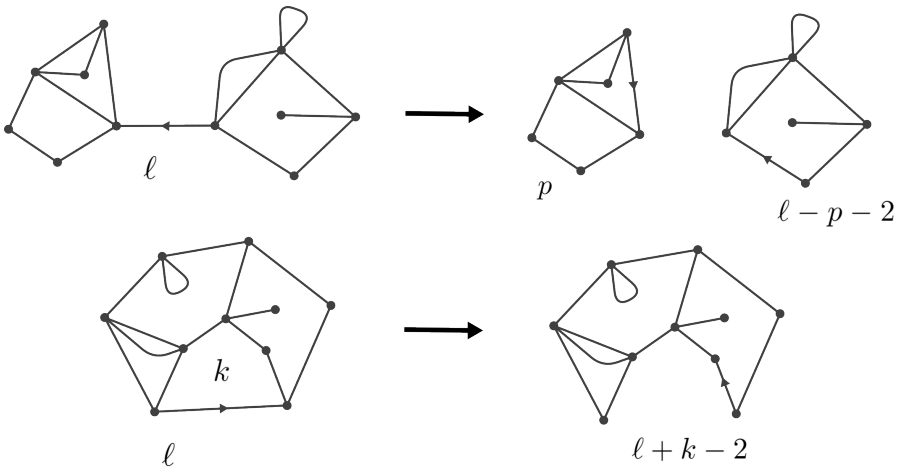

Figure 2.5: Two cases of removing the root edge of a disk. On the top one, we are left with two maps of length p and $\ell - p - 2$ for a $0 \leq p \leq \ell - 2$. On the bottom one, the new map contains one face less, and the boundary length is now $\ell + k - 2$ for any $k \geq 0$.

Let us discuss the two cases, where we both start with a map of perimeter ℓ. If by removing the root edge we end up with two maps, these maps will have new perimeters

p and $\ell - p - 2$, because the removed edge contributed 2 in boundary length. Here, we take that the map which the rooting points to has perimeter p. This holds for $0 \leq p \leq \ell - 2$, as we can have that $p = 0$, where we end up with one map having only one vertex, all the way up to $p = \ell - 2$, where again we are left with a map with one vertex. In the other case, removing the root edge results in a map with one face less. Say the face on the left of the root edge has degree $k \geq 1$. After removing the root edge, k becomes $k - 1$ and ℓ becomes $\ell - 1$, as the removed edge contributed 1 in the face degrees k and ℓ. Adding these lengths gives us the new boundary length $\ell + k - 2$.
Put into a recurrence relation, this results in Tutte's famous *loop equation*

$$W^{(\ell)} = \sum_{k=1}^{\infty} q_k W^{(l+k-2)} + \sum_{p=0}^{l-2} W^{(p)} W^{(l-p-2)}. \tag{2.7}$$

To solve this, Let us introduce a new generating variable x for the boundary length ℓ, allowing us to establish the following generating functions,

$$W(x) := \sum_{l=0}^{\infty} W^{(\ell)} x^{-\ell-1}, \qquad V'(x) = x - \sum_{k=1}^{\infty} q_k x^{k-1}. \tag{2.8}$$

With these, we can see the Tutte equation to be equivalent to

$$V'(x)W(x) - W(x)^2 = Q(x) := t - \sum_{p=0}^{\infty} x^p \sum_{k=p+2}^{\infty} q_k W^{(k-p-2)}. \tag{2.9}$$

Which has the solution

$$W(x) = \frac{1}{2}\left(V'(x) - \sqrt{V'(x)^2 - 4Q(x)}\right). \tag{2.10}$$

2.4.1 The disk function

An explicit expression for the disk function $W^{(\ell_1)}$ of bipartite maps with boundary length $2\ell_1$ is given in [6] via

$$W^{(\ell_1)}(t, \mathbf{q}) = \binom{2\ell_1}{\ell_1} \int_0^R dr\, g'_{\mathbf{q}}(r) r^{\ell_1}, \tag{2.11}$$

where

$$g_{\mathbf{q}}(r) = r - \sum_{k=1}^{\infty} q_k \frac{1}{2} \binom{2k}{k} r^k, \tag{2.12}$$

and $R = R(t, \mathbf{q})$ is defined by $g_{\mathbf{q}}(R) = t$.

2.4.2 The cylinder function and beyond

In disks, we can also have holes of certain boundary lengths. To give an expression for the generating function of bipartite maps with n boundaries, we can use the equation from [11]

$$W^{(\ell_1,\ldots,\ell_n)}(t, \mathbf{q}) = 2\ell_n \frac{\partial W^{(\ell_1,\ldots,\ell_{n-1})}}{\partial q_{\ell_n}}. \tag{2.13}$$

For the cylinder function ($n = 2$) with boundaries $2\ell_1$ and $2\ell_2$, we insert what we know, i.e. $W^{(\ell_1)}(t, \mathbf{q})$, to get the explicit expression

$$W^{(\ell_1,\ell_2)}(t, \mathbf{q}) = \frac{\ell_1 \ell_2}{\ell_1 + \ell_2} \binom{2\ell_1}{\ell_1} \binom{2\ell_2}{\ell_2} R^{\ell_1+\ell_2}. \tag{2.14}$$

These cylinders have a root edge somewhere on both boundaries. We can have arbitrarily many holes and we can use (2.13) repeatedly to obtain generating functions for these cases.

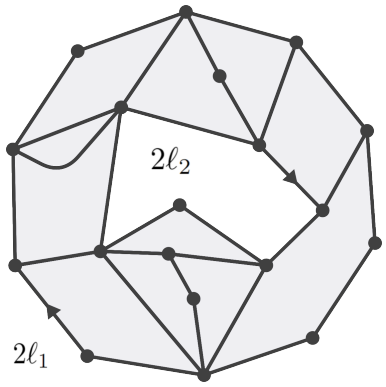

Figure 2.6: A rooted bipartite cylinder with boundary lengths $2\ell_1$ and $2\ell_2$.

3 Labelled Quadrangulations

In this thesis, we are interested in coupling 2D Quantum Gravity to a scalar field. To add a scalar field to a planar map, one can label the vertices with integer values, which can be seen as a discretization of the scalar field. We do need to impose some conditions for this scalar field, like a restriction on the gradient, but those will be introduced later.

3.1 Labelled maps

Definition 3.1. A *labeled map* is a map where we assign an integer value to every vertex. In particular, a *labeled quadrangulation* is a labeled map where all faces are of degree four.

When we now restrict neighboring vertices to differ by ± 1, there are two possibilities of what each face looks like. Either the four labels of the face can have two distinct values, which we call non-colorful labeling, or the four labels can have three distinct values, called colorful labeling. It is exactly this colorful labeling that we will decorate our quadrangulations with.

Definition 3.2. A *colorfully labeled quadrangulation* is a labeled quadrangulation where every face has three distinct labels: ℓ, $\ell + 1$, and $\ell + 2$ (for some $\ell \in \mathbb{Z}$).

Remark. Labeling the quadrangulations changes the counting problem. We still have all possible unlabeled quadrangulations, but there are (almost always) multiple ways to label these. This is why our geometry changes, as we stated in Section 1.

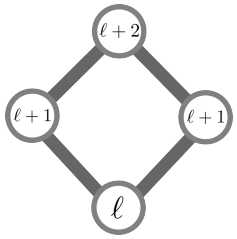

Figure 3.1: A colorfully labeled face of a quadrangulation.

3.2 Convenient model

We will now define the model we will be working with. This choice of model is convenient, as it allows a useful decomposition and has an interesting bijection to rigid quadrangulations, which we will not go into detail about. In the following subsection, we will see this *'gasket' decomposition* and why it is so useful. With this model, we expect to be in the universality class of $\mathrm{LQG}_{\gamma=2}$.

Definition 3.3. The *labeled quadrangulations* $\mathfrak{q}$ we will look at are disks and have the following restriction imposed:

- The boundary length is 2ℓ;
- The labels on the boundary are alternatingly 0, 1, 0, 1;
- Neighboring vertices differ by ± 1;
- The quadrangulations are colorful;
- The root edge lies on the boundary and points from a 0 to a 1.

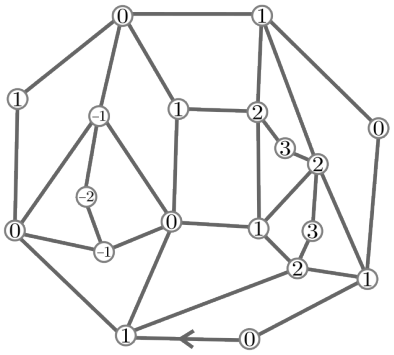

Figure 3.2: An example of a labeled quadrangulation.

From now on, when stating *labeled quadrangulation*, we refer to this model unless explicitly indicated differently.

3.2.1 Gasket decomposition

The method of gasket decomposition has extensively been used in [12, 13, 14] and has proven useful. It decomposes maps into a cluster (which we will call *gasket*) containing the root edge and then aims to describe what happens inside the faces of this gasket. It formulates the enumeration problem in terms of Boltzmann planar maps, where the gasket is the map, and its faces receive a certain weight for what can be inside based on its degree. This is useful, as we understand the combinatorics of Boltzmann maps well. Let us define gaskets in the context of labeled quadrangulations.

Definition 3.4. The *gasket* $g(\mathfrak{q})$ of a labeled quadrangulation $\mathfrak{q}$ is the connected component containing the boundary root consisting of all edges that connect the values of the two endpoints of the boundary root. For the initial gasket these are 0 and 1.

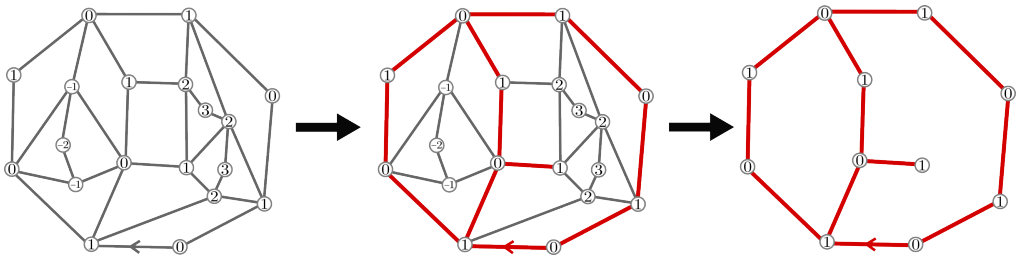

Figure 3.3: Highlighting the gasket of a labeled quadrangulation where all zeros and ones form a connected component depicted in red.

We can see that this gasket $g(\mathfrak{q})$, is again a disk. The disk function we saw in Section 2.4 enumerates disks as Boltzmann maps. Suppose now we specify the weight of the faces for everything that can happen inside. In that case, we can derive a relation between the disk function and the generating function of labeled quadrangulations.

3.2.2 Level sets

Due to this gasket decomposition, level sets arise. These are loops that cross all edges in a gasket that go from 0 to -1, or from 1 to 2. When jumping over a level set, you go from the gasket face boundary to a new boundary of either $-1, -2$-vertices or $2, 3$-vertices. Inside these new boundaries, we can have all kinds of labeled quadrangulations again, where the boundaries will be part of the new gasket. This forms the basis for setting up a recurrence relation later. Jumping over a level set essentially means that you go from a $(x, x+1)$-gasket to either a $(x+2, x+3)$-gasket or a $(x-2, x-1)$-gasket (for $x \in 2\mathbb{Z}$), and so on. This is particularly important when determining a statistical distribution of the labels.

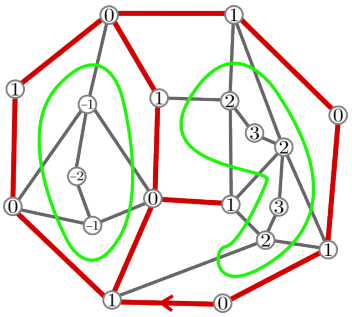

Figure 3.4: Explicit example of the level sets (green loops) in the example quadrangulation.

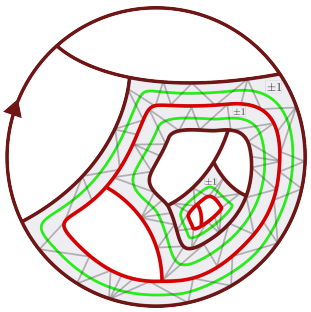

Figure 3.5: A rough outline of a random labeled quadrangulation to see what happens deeper inside a gasket face. Inside a gasket face, you cross a level set and end up on a new gasket, either ± 1 in value. The different coloring of the gaskets serves solely to distinguish the gaskets better.

3.3 Connection to the disk function

We will now establish the relation between labeled quadrangulations and the disk function for Boltzmann maps, which is based on an exercise sheet of Budd [11]. Let us introduce a generating function $Q^{(\ell)}(v)$ for the labeled quadrangulations of boundary length ℓ,

$$Q^{(\ell)}(v) = \sum_{n=0}^{\infty} a_n v^n, \tag{3.1}$$

where a_n is the number of labeled quadrangulations with n vertices. This can be seen to be equivalent to

$$Q^{(\ell)}(v) = \sum_{\substack{\text{labelled} \\ \text{quadrangulations } \mathfrak{q} \\ \text{of perimeter } 2\ell}} v^{|V(\mathfrak{q})|}, \tag{3.2}$$

where $Q^{(0)} = v$ by convention, being the map that consists of only one vertex. We can then split the summation and rewrite it as

$$Q^{(\ell)}(v) = \sum_{\substack{\mathfrak{m} \in \mathcal{M} \text{ with} \\ \text{perimeter } 2\ell}} \sum_{\substack{\text{labelled} \\ \text{quadrangulations } \mathfrak{q} \\ \text{of perimeter } 2\ell \\ g(\mathfrak{q})=\mathfrak{m}}} v^{|V(\mathfrak{q})|}. \tag{3.3}$$

What then remains to be done is to assign a correct weight $q_k(v)$ to all the gasket faces, such that we get the relation

$$\sum_{\substack{\text{labelled} \\ \text{quadrangulations } \mathfrak{q} \\ \text{of perimeter } 2l \\ g(\mathfrak{q})=\mathfrak{m}}} v^{|V(q)|} = \prod_{f \in F(\mathfrak{m}) \setminus \{f_r\}} q_{\deg f/2}. \tag{3.4}$$

This way, the relation between the disk function and labeled quadrangulations will be established as

$$Q^{(\ell)}(v) = W^{(\ell)}(v, q_k(v)) = \sum_{\substack{\mathfrak{m} \in \mathcal{M} \text{ with} \\ \text{perimeter } 2\ell}} \prod_{f \in F(\mathfrak{m}) \setminus \{f_r\}} q_{\deg f/2}(v). \tag{3.5}$$

Let us first note that the gasket faces are independent. Therefore, we see this product over the face weights. Let us now pick a face of the gasket of arbitrary perimeter $2k$ and start at a 0-vertex, which always has a face adjacent to it. Going from a neighboring 1-vertex to a new 2-vertex (as a 0-vertex would belong to the gasket) and completing the face adjacent to the 0-vertex, we draw an edge from the 2 to the 1 on the other side of the 0, creating a face. Here, you can also use the 2-vertex from a previous time. We do this until all edges of the gasket face boundary have a face next to them. From all 1-vertices of the gasket adjacent to the newly formed face in the middle, we can have arbitrarily many extra edges going from 1 to 2. Since we need the quadrangles to be colorfully labeled, these 2-vertices need to be connected via 3-vertices. By doing this, we end up with a new perimeter alternatingly $2, 3, 2, 3$, which is now again the boundary of a labeled quadrangulation, but with a $2, 3$-boundary (which are, of course, in bijection with ordinary labeled quadrangulations by shifting all vertices by -2). The crucial thing to notice is that we have now returned to our original problem with a new boundary length $2p$, for any $p \geq 0$, in which we again have a gasket whose faces share the same process described above and seen in Figure 3.6.

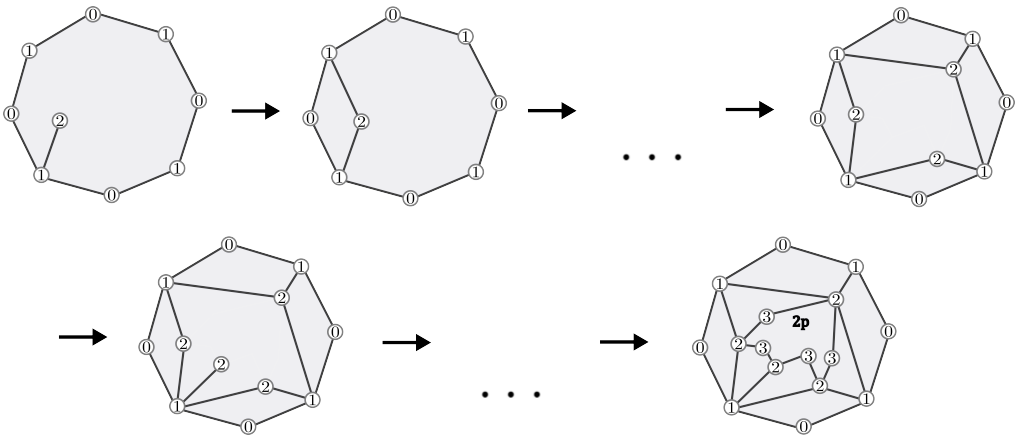

Figure 3.6: A step-by-step visualization of a possible construction of a gasket face of length 8 as described in Section 3.3. In the last step, a new boundary of length $2p$ is formed, in which we return to a labeled quadrangulation but now with boundary values alternating $2, 3, 2, 3$. The dots represent the omitted steps.

We can thus already establish the following formula for the weight of a gasket face,

$$q_k(v) := \sum_{p=0}^{\infty} \alpha Q^{(p)}(v), \tag{3.6}$$

where α denotes the number of possible ways to go from a gasket face of perimeter $2k$ to a boundary length $2p$, and we take the sum over all $p \geq 0$. To figure out the value of α, we will take an arbitrary gasket 'ring'. In Figure 3.5, these are all faces that a level set crosses. We then proceed by cutting open one of the edges and laying it out, of which an example can be seen in Figure 3.7

We start with a gasket face of perimeter $2k$, created by k quadrangles (the bottom line of quadrangles in Figure 3.7). To go to a new boundary length of $2p$, we must distribute p faces over k spots. The number of possibilities to put p faces in k spots is (stars and bars problem)

$$\binom{p+k-1}{p}.$$

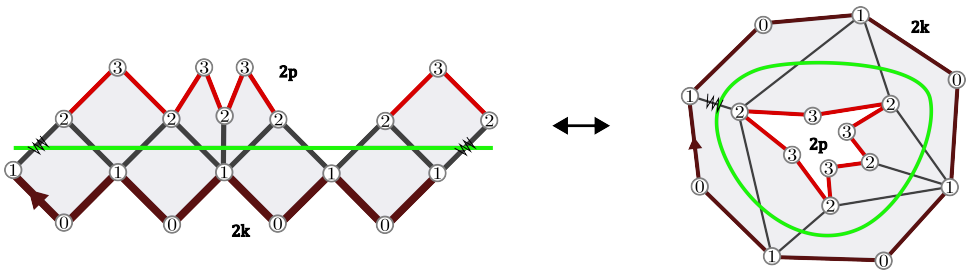

Figure 3.7: An example of a cut-open gasket ring and the corresponding gasket face. Here, $2k = 8$ and $2p = 8$.

Lastly, we note that we can either go from a 1 to a 2 or from a 0 to a -1, giving us a factor 2. All in all, the face weight becomes

$$q_k(v) := 2\sum_{p=0}^{\infty} \binom{p+k-1}{p} Q^{(p)}(v). \tag{3.7}$$

Giving us the relation

$$Q^{(\ell)}(v) = W^{(\ell)}(v, q_k(v)). \tag{3.8}$$

Using now the disk function and the corresponding potential,

$$W(x) = \sum_{\ell=0}^{\infty} W^{(\ell)} x^{-2\ell-1}, \qquad V'(x) = x - \sum_{k=1}^{\infty} q_k x^{2k-1}, \tag{3.9}$$

we can establish the relation

$$1 - \frac{V'(x)}{x} = 2\frac{W\left(\sqrt{1-x^2}\right)}{\sqrt{1-x^2}}. \tag{3.10}$$

To see this, let us first look at the left-hand side,

$$1 - \frac{V'(x)}{x} = \sum_{k=1}^{\infty} q_k x^{2k-2}. \tag{3.11}$$

Substituting now the face weight (3.7), we obtain

$$1 - \frac{V'(x)}{x} = 2\sum_{k=1}^{\infty}\sum_{p=0}^{\infty} \binom{p+k-1}{p} Q^{(p)} x^{2k-2}. \tag{3.12}$$

Now we look at the right-hand side and use that

$$W(x) = \sum_{\ell=0}^{\infty} Q^{(\ell)} x^{-2\ell-1}, \tag{3.13}$$

as $Q^{(\ell)}(v) = W^{(\ell)}(v, q_k(v))$. We then have

$$2\frac{W\left(\sqrt{1-x^2}\right)}{\sqrt{1-x^2}} = \frac{2}{\sqrt{1-x^2}}\sum_{\ell=0}^{\infty} Q^{(\ell)}\left(\sqrt{1-x^2}\right)^{-2\ell-1} \tag{3.14}$$

$$= 2\sum_{\ell=0}^{\infty} Q^{(\ell)}(1-x^2)^{-\ell-1} \tag{3.15}$$

$$= 2\sum_{\ell=0}^{\infty} Q^{(\ell)}\sum_{p=0}^{\infty}\binom{p+\ell}{p}x^{2p} \tag{3.16}$$

$$= 2\sum_{\ell=0}^{\infty}\sum_{p=0}^{\infty}\binom{p+\ell}{p}Q^{(\ell)}x^{2p}. \tag{3.17}$$

This is equivalent to

$$2\sum_{\ell=0}^{\infty}\sum_{p=0}^{\infty}\binom{\ell+p}{\ell}Q^{(\ell)}x^{2p}, \tag{3.18}$$

because

$$\binom{p+\ell}{p} = \frac{(p+\ell)!}{p!(\ell+p-p)!} = \frac{(p+\ell)!}{(p+\ell-\ell)!\ell!} = \binom{\ell+p}{\ell}. \tag{3.19}$$

Going from (3.15) to (3.16), we used that

$$\frac{1}{(1-x^2)^{\ell+1}} = \sum_{p=0}^{\infty}\binom{p+\ell}{p}x^{2p}. \tag{3.20}$$

Setting now $\ell = k-1$, we obtain

$$2\sum_{k=1}^{\infty}\sum_{p=0}^{\infty}\binom{p+k-1}{p}Q^{(p)}x^{2k-2}, \tag{3.21}$$

which is the same as (3.12). Therefore, we now have

$$1-\frac{V'(x)}{x} = 2\frac{W\left(\sqrt{1-x^2}\right)}{\sqrt{1-x^2}}. \tag{3.22}$$

Hence, we see that $(W(x)-\frac{1}{2}V'(x))/x$ is symmetric under $x \to \sqrt{1-x^2}$.

3.4 Branch cut

From Section 2.4, we know that the solution of the disk function is

$$W(x) = \frac{1}{2}\left(V'(x) - \sqrt{V'(x)^2 - 4Q(x)}\right). \tag{3.23}$$

If we assume now that only finitely many q_k are nonzero, $V'(x)$ and $Q(x)$ are polynomials. Consequently, we can make the *one-cut assumption* that $V'(x)^2 - 4Q(x)$ factorizes as

$$V'(x)^2 - 4Q(x) = M(x)^2(x-c_+)(x-c_-), \qquad (c_- < c_+) \tag{3.24}$$

where we take the sign of $M(x)$ such that $V'(x)/(xM(x)) \to 1$ as $x \to 1$. The disk function now becomes

$$W(x) = \frac{1}{2}\left(V'(x) - M(x)\sqrt{(x-c_+)(x-c_-)}\right). \qquad (x \in \mathbb{C}\setminus[c_-,c_+]) \tag{3.25}$$

The interval $[c_-, c_+] \in \mathbb{R}$ is called the *branch cut*, and $W(x)$ is not analytic there. The gasket of the quadrangulations is *bipartite*, which implies that the branch cut $[c_-, c_+]$ is symmetric around 0, because $xW(x)$ is even in x. Using the notation $R = \frac{1}{4}c_+^2 = \frac{1}{4}c_-^2$ $(R > 0)$, we get that $c_+ = 2\sqrt{R} = -c_-$. Substituting this in $W(x)$, we obtain

$$W(x) = \frac{1}{2}\left(V'(x) - M(x)\sqrt{x^2 - 4R}\right). \tag{3.26}$$

Rearranging and dividing by x, we get

$$2\left(\frac{W(x) - \frac{1}{2}V'(x)}{x}\right) = -M(x)\sqrt{1 - \frac{4R}{x^2}}. \tag{3.27}$$

For the left-hand side, we derived that it is symmetric under $x \to \sqrt{1-x^2}$. Therefore a natural guess for $M(x)$ is

$$M(x) = \sqrt{1 - \frac{4R}{1-x^2}}. \tag{3.28}$$

Leaving us with the final expression

$$2\left(\frac{W(x) - \frac{1}{2}V'(x)}{x}\right) = -\sqrt{1 - \frac{4R}{1-x^2}}\sqrt{1 - \frac{4R}{x^2}}. \tag{3.29}$$

To verify this, one could compute the coefficient $Q^{(\ell)} = [x^{-2\ell-1}]W(x)$ and compare with explicit formulas, found in [15].

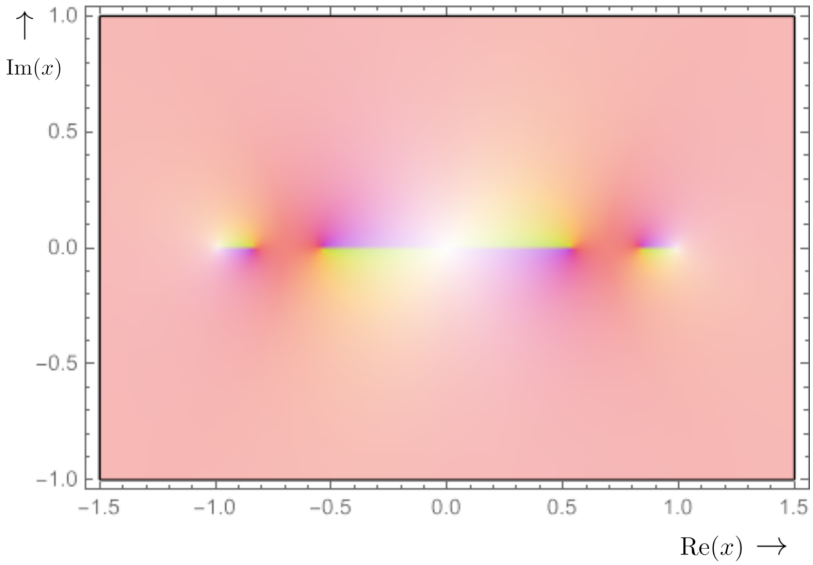

Figure 3.8: The branch cut of (3.29) for $4R = 0.3$ (subcritical). The branch cut of $W(x)$ is the middle part $[-2\sqrt{R}, 2\sqrt{R}] \approx [-0.5, 0.5]$.

3.5 Criticality

In Section 2.3.1, we briefly mentioned criticality. For criticality of the gasket, $M(x)$ should be 0 for $x = 2\sqrt{R}$ [11]. From (3.28), we then get that $R = 1/8$. To get the

critical value for the vertex weight v, we can set up the generating function for v. Firstly, we have that

$$W(x) = \sum_{n=0}^{\infty} Q^{(\ell)} x^{-2\ell-1}. \tag{3.30}$$

We also know that $W^{(0)} = v$ by convention. Hence, $v = [x^{-1}]W(x)$. As $V'(x)$ only has positive powers of x, we can apply this to (3.29), such that

$$v = [x^{-2}] \left(\frac{W(x) - \frac{1}{2}V'(x)}{x} \right) \tag{3.31}$$

The expression on the right can be derived further as

$$\left(\frac{W(x) - \frac{1}{2}V'(x)}{x} \right) = -\frac{1}{2}\sqrt{1 - \frac{4R}{1-x^2}}\sqrt{1 - \frac{4R}{x^2}} \tag{3.32}$$

$$= -\frac{1}{2}\sqrt{1 - \frac{4R}{1-x^2} - \frac{4R}{x^2} + \frac{16R^2}{x^2(1-x^2)}} \tag{3.33}$$

$$= -\frac{1}{2}\sqrt{1 - \frac{4R(1-4R)}{x^2(1-x^2)}} \tag{3.34}$$

$$= -\frac{1}{2}\sqrt{1 - \frac{4\tilde{R}}{x^2(1-x^2)}}, \tag{3.35}$$

where $\tilde{R} = R(1-4R)$. Expanding this for $\tilde{R}$ small, we get for v that

$$v = [x^{-2}] - \frac{1}{2}\sum_{n=0}^{\infty} \frac{(-1)^{n-1}}{4^n(2n-1)} \binom{2n}{n} \left(\frac{-4\tilde{R}}{x^2(1-x^2)} \right)^n \tag{3.36}$$

$$= [x^{-2}] \sum_{n=0}^{\infty} \frac{1}{2(2n-1)} \binom{2n}{n} \tilde{R}^n \frac{1}{x^{2n}(1-x^2)^n}. \tag{3.37}$$

The index $n = 0$ yields 1, therefore we can set $n \to n+1$, such that we are left with

$$[x^{-2}] \sum_{n=0}^{\infty} \frac{1}{2(2n+1)} \binom{2n+2}{n+1} \tilde{R}^{n+1} \frac{1}{x^{2n+2}(1-x^2)^{n+1}}. \tag{3.38}$$

Using that both

$$\frac{1}{2(2n+1)} \binom{2n+2}{n+1} = \frac{1}{2(2n+1)} \frac{(2n+2)(2n+1)}{(n+1)(n+1)} \binom{2n}{n} = \frac{1}{n+1} \binom{2n}{n}, \tag{3.39}$$

and

$$\frac{1}{(1-x^2)^{n+1}} = \sum_{p=0}^{\infty} \binom{p+n}{p} x^{2p}, \tag{3.40}$$

we get

$$v = \sum_{n=0}^{\infty} \frac{1}{n+1} \binom{2n}{n} \tilde{R}^{n+1} [x^{-2}] \sum_{p=0}^{\infty} \binom{p+n}{p} \frac{x^{2p}}{x^{2n+2}}. \tag{3.41}$$

The coefficient of x^{-2} is obtained from the sum for $p = n$. This gives us the final expression

$$v = \sum_{n=0}^{\infty} \frac{1}{n+1} \binom{2n}{n}^2 \tilde{R}(v)^{n+1}. \tag{3.42}$$

Analogously,

$$Q^{(\ell)}(v) = \sum_{n=0}^{\infty} \frac{1}{n+1} \binom{2n}{n} \tilde{R}^{n+1} [x^{-2\ell-2}] \sum_{p=0}^{\infty} \binom{p+n}{p} \frac{x^{2p}}{x^{2n+2}} \tag{3.43}$$

$$= \sum_{n=0}^{\infty} \frac{1}{n+1} \binom{2n}{n} \binom{2n-\ell}{n-\ell} \tilde{R}(v)^{n+1} \tag{3.44}$$

$$= \sum_{n=\ell}^{\infty} \frac{1}{n+1} \binom{2n}{n} \binom{2n-\ell}{n} \tilde{R}(v)^{n+1} \tag{3.45}$$

The critical value for this sum (3.42) is $\tilde{R}(v_*) = 1/16$, from which we get that $v_* = 1/4\pi$. For R, the critical value is $R(v_*) = 1/8$. This result is also confirmed by [15].

3.5.1 Critical exponent

Definition 3.5. The *critical exponent* α defines the asymptotic behaviour of $W^{(\ell)}$. As $\ell \to \infty$, $W^{(\ell)}$ scales as $W^{(\ell)} \sim C^\ell \ell^{-\alpha-\frac{1}{2}}$ for a $C > 0$.

Using our results from the previous sections, we can find the critical exponent of $W^{(\ell)}$, and hence also for $Q^{(\ell)}$. We know that

$$W^{(\ell)} = [x^{-2\ell-1}]W(x) \tag{3.46}$$

$$= [x^{-2\ell-1}] \left(W(x) - \frac{1}{2} V'(x) \right) \tag{3.47}$$

$$= [x^{-2\ell-1}] - \frac{x}{2} \sqrt{1 - \frac{4R}{1-x^2}} \sqrt{1 - \frac{4R}{x^2}} \tag{3.48}$$

$$= [x^{-2\ell-2}] - \frac{1}{2} \sqrt{1 - \frac{4R}{1-x^2}} \sqrt{1 - \frac{4R}{x^2}}. \tag{3.49}$$

Setting the critical value $R(v_*) = 1/8$ and using Cauchy's integral formula, we get

$$W^{(\ell)} = -\frac{1}{2} \frac{1}{2\pi i} \oint_{\mathscr{C}} dx \; x^{2\ell+1} \sqrt{1 - \frac{\frac{1}{2}}{1-x^2}} \sqrt{1 - \frac{\frac{1}{2}}{x^2}}, \tag{3.50}$$

where the contour $\mathscr{C}$ is the contour around the branch cut, seen in Figure 3.9. Substituting

$$x = \frac{1}{\sqrt{2}} e^{i\theta}, \qquad x^2 = \frac{1}{2} e^{2i\theta}, \qquad dx = \frac{i}{\sqrt{2}} e^{i\theta} d\theta, \tag{3.51}$$

yields

$$W^{(\ell)} = -\frac{1}{4\pi} \left(\frac{1}{2} \right)^{\ell+1} \int_0^{2\pi} d\theta \; e^{(2\ell+2)i\theta} \sqrt{1 - \frac{1}{2 - e^{2i\theta}}} \sqrt{1 - \frac{1}{e^{2i\theta}}} \tag{3.52}$$

$$= -\frac{1}{4\pi} \left(\frac{1}{2} \right)^{\ell+1} \int_0^{2\pi} d\theta \; e^{(2\ell+2)i\theta} \sqrt{\frac{(1 - e^{2i\theta})(1 - e^{-2i\theta})}{2 - e^{2i\theta}}}. \tag{3.53}$$

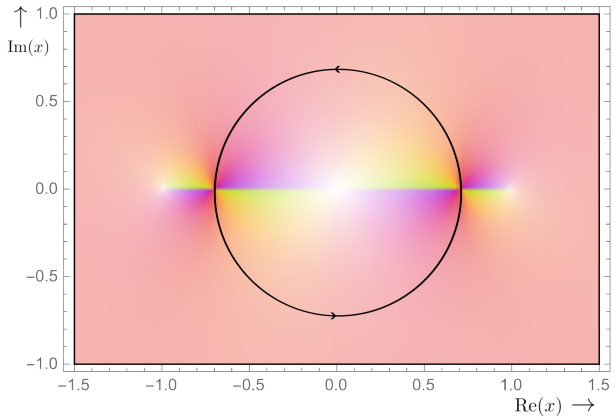

Figure 3.9: The contour $\mathscr{C}$ around the branch cut of $W(x)$ for the critical value $R = 1/8$, which is $[-\frac{1}{\sqrt{2}}, \frac{1}{\sqrt{2}}]$.

The numerator of the fraction in the square root can be written as

$$\sqrt{(1-e^{2i\theta})(1-e^{-2i\theta})} = \sqrt{2-(e^{2i\theta}+e^{-2i\theta})} \tag{3.54}$$
$$= \sqrt{2-2\cos(2\theta)} \tag{3.55}$$
$$= \sqrt{4\sin^2(\theta)} \tag{3.56}$$
$$= 2|\sin(\theta)|, \tag{3.57}$$

such that

$$W^{(\ell)} = -\frac{1}{4\pi}\left(\frac{1}{2}\right)^{\ell}\int_0^{2\pi} d\theta\; e^{(2\ell+2)i\theta}\frac{|\sin(\theta)|}{\sqrt{2-e^{2i\theta}}} \tag{3.58}$$
$$= -\frac{1}{2\pi}\left(\frac{1}{2}\right)^{\ell}\int_0^{\pi} d\theta\; e^{(2\ell+2)i\theta}\frac{e^{i\theta}-e^{-i\theta}}{i\sqrt{2-e^{2i\theta}}} \tag{3.59}$$
$$= \frac{1}{2\pi}\left(\frac{1}{2}\right)^{\ell} i\int_0^{\pi} d\theta\; e^{(2\ell+1)i\theta}\frac{e^{2i\theta}-1}{\sqrt{1-(e^{2i\theta}-1)}}. \tag{3.60}$$

As we look at ℓ very large, we get the largest influence from θ very small. For $\theta \to 0$,

$$e^{2i\theta} - 1 \approx 2i\theta + \mathcal{O}(\theta^2). \tag{3.61}$$

Therefore, we can use the Maclaurin series for x small

$$\frac{x}{\sqrt{1-x}} \approx x + \mathcal{O}(x^2). \tag{3.62}$$

We are then left with

$$W^{(\ell)} \approx \frac{1}{2\pi}\left(\frac{1}{2}\right)^{\ell} i\int_0^{\pi} d\theta\; e^{(2\ell+1)i\theta}(e^{2i\theta}-1) \tag{3.63}$$
$$= \frac{1}{2\pi}\left(\frac{1}{2}\right)^{\ell} i\int_0^{\pi} d\theta\; \left(e^{(2\ell+3)i\theta} - e^{(2\ell+1)i\theta}\right). \tag{3.64}$$

Integrating this gives[3]

[3]If we had used more terms of the Maclaurin series (3.62), they would give contributions of $\ell^{-3}, \ell^{-4}, \ldots$, which are dominated by ℓ^{-2} for large ℓ.

$$W^{(\ell)} \approx \frac{1}{4\pi}\left(\frac{1}{2}\right)^{\ell} \frac{1}{\ell^2 + 2\ell + \frac{3}{4}}. \tag{3.65}$$

For $\ell \to \infty$, we have the asymptotic behavior

$$W^{(\ell)} \sim \frac{1}{4\pi} 2^{-\ell} \ell^{-2}. \tag{3.66}$$

Therefore, the gasket is non-generic critical with exponent $\alpha = 3/2$.

4 Marking a vertex

To actually obtain a distribution of the value of the labels, we will mark one of the vertices of the quadrangulation and get a probability distribution of the value of this uniformly marked vertex.

4.1 Pointed labelled quadrangulations

Definition 4.1. Let us start by defining what we mean by pointing a map. A *pointed labeled rooted planar map* is a labeled rooted planar map where one vertex is marked uniformly at random.

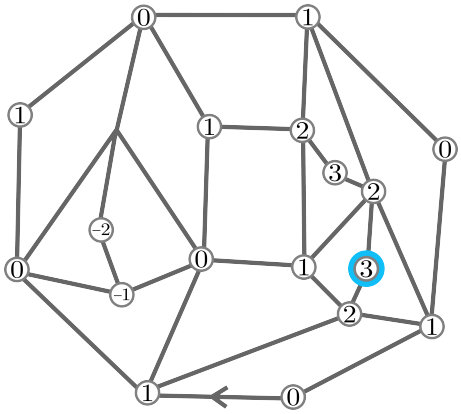

Figure 4.1: A pointed labeled quadrangulation, where the vertex surrounded by a blue ring is the (uniformly at random) marked vertex

The generating function of these pointed labeled quadrangulations is then

$$Q_\bullet^{(\ell)}(v) = \sum_{\substack{\text{pointed labelled} \\ \text{quadrangulations } \mathfrak{q} \\ \text{of perimeter } 2\ell}} v^{|V(\mathfrak{q})|}. \tag{4.1}$$

It is very similar to counting just labeled quadrangulations, but for every quadrangulation, we now have $|V(\mathfrak{q})|$ possibilities. In giving a weight to a quadrangulation, we do not count the pointed vertex. Therefore, one can observe that $Q_\bullet^{(\ell)}(v)$ is the derivative over v of $Q^{(\ell)}(v)$,

$$Q_\bullet^{(\ell)}(v) = \frac{\partial}{\partial v} Q^{(\ell)}(v). \tag{4.2}$$

We take again the generating variable x for boundary length and define

$$Q_\bullet(x) := \sum_{\ell=0}^{\infty} x^{-\ell-1} Q_\bullet^{(\ell)}, \qquad q_\bullet(x) := \sum_{k=1}^{\infty} x^{k-1} q_k^\bullet,$$

where

$$q_k^\bullet = \frac{\partial}{\partial v} q_k = 2 \sum_{p=0}^{\infty} \binom{p+k-1}{p} Q_\bullet^{(p)}(v). \tag{4.3}$$

Note that, in contrast to the definitions of $W(x)$ and $V'(x)$, for convenience, we use x linearly and not quadratically. Therefore, the branch cut of $Q_\bullet(x)$ is $[0, 1/2]$ for the critical case, where $W(x)$ had a branch cut at $[-1/\sqrt{2}, 1/\sqrt{2}]$. As a reminder, we had

$$W(x) = \sum_{\ell=0}^{\infty} x^{-2\ell-1} W^{(\ell)}, \qquad V'(x) = x - \sum_{k=1}^{\infty} x^{2k-1} q_k. \tag{4.4}$$

Differentiating these with respect to v, we obtain the following,

$$\frac{\partial W(x)}{\partial v} = \sum_{\ell=0}^{\infty} x^{-2\ell-1} W_\bullet^{(\ell)} = x Q_\bullet(x^2), \tag{4.5}$$

$$\frac{\partial V'(x)}{\partial v} = -\sum_{k=1}^{\infty} x^{2k-1} q_k^\bullet = -x q_\bullet(x^2). \tag{4.6}$$

Using now the relation between $W(x)$ and $V'(x)$,

$$1 - \frac{V'(x)}{x} = 2\frac{W\left(\sqrt{1-x^2}\right)}{\sqrt{1-x^2}}, \tag{4.7}$$

we can derive a relation for $Q_\bullet(x)$ and $q_\bullet(x)$

$$-\frac{1}{x}\frac{\partial V'(x)}{\partial v} = \frac{2}{\sqrt{1-x^2}}\frac{\partial W(\sqrt{1-x^2})}{\partial v} \tag{4.8}$$

$$\frac{x q_\bullet(x^2)}{x} = 2\frac{\sqrt{1-x^2}}{\sqrt{1-x^2}} Q_\bullet(1-x^2), \tag{4.9}$$

$$q_\bullet(x^2) = 2Q_\bullet(1-x^2). \tag{4.10}$$

This is equivalent to

$$q_\bullet(x) = 2Q_\bullet(1-x) \tag{4.11}$$

for $x^2 \to x$.

(4.12)

4.1.1 Pointed disk function

In section 2.4.1, we saw the explicit expression of $W^{(\ell)}$. For the pointed disk function, we then have

$$W_\bullet^{(\ell)} = \frac{\partial}{\partial t} W^{(\ell)}, \qquad W_\bullet(x) = \sum_{\ell=0}^{\infty} W_\bullet^{(\ell)} x^{-2\ell-1} = \frac{\partial}{\partial t} W(x). \tag{4.13}$$

From [6], we get an explicit expression for this,

$$W_\bullet(x) = \frac{1}{\sqrt{(x-c_+)(x-c_-)}}. \tag{4.14}$$

We work with quadrangulations, which are bipartite maps, such that $c_+ = 2\sqrt{R} = -c_-$. Therefore, this changes to

$$W_\bullet(x) = \frac{1}{\sqrt{x^2 - 4R}}, \tag{4.15}$$

from which can be deduced by series expansion around $x \to \infty$ that

$$W_\bullet^{(2\ell)} = \binom{2\ell}{\ell} R^\ell. \tag{4.16}$$

However, as stated earlier we will work with x linearly. Therefore, we redefine $W_\bullet(x)$ to be

$$W_\bullet(x) = \sum_{\ell=0}^{\infty} W_\bullet^{(2\ell)} x^{-\ell-1} = \sum_{\ell=0}^{\infty} \binom{2\ell}{\ell} R^\ell x^{-\ell-1} = \frac{1}{\sqrt{x(x-4R)}}, \tag{4.17}$$

where ℓ is the half perimeter, as we want it to be, since the boundary lengths are even (2ℓ).

4.2 Setting a recurrence relation

To set an equation which $Q_\bullet^{(\ell)}(v)$ satisfies, we can find a recurrence relation using the gasket decomposition. On the left-hand side of the equation, we put $Q_\bullet^{(\ell)}(v)$, the generating function for our pointed labeled quadrangulations. Let us now think of the two possibilities the pointed vertex can be. This is either on the gasket or inside one of the gasket faces. If it lies on the $(x, x+1)$-gasket (for a $x \in 2\mathbb{Z}$), we can see the gasket to be a pointed disk with the gasket as the map, so we will use the pointed disk function for this possibility. If it lies inside one of the gasket faces, we can see the gasket inside this face again as a pointed labeled quadrangulation with now either a $(x-2, x-1)$-boundary or a $(x+1, x+2)$-boundary. We need to consider all possible ways this can happen. So, say the gasket face in which the marked vertex lies is of degree $2k$. We can observe that, briefly disregarding the face itself, we obtain a cylinder. The number of cylinders of perimeters 2ℓ and $2k$ is given by the cylinder function we saw in Section 2.4.2. However, this considers all the ways the inner boundary of length $2k$ can be rooted, and we can take this rooting in some arbitrary fashion, such as closest to the original root. Therefore, we divide the cylinder function by $2k$. See Figure 4.2 for a rough sketch of this process.

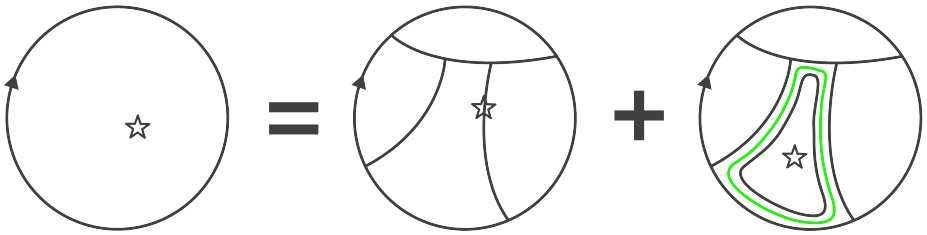

Figure 4.2: Rough outline of the two possibilities of where the marked vertex can be.

Writing out the equation in shorthand, we get

$$Q_\bullet^{(\ell)} = W_\bullet^{(2\ell)} + \sum_{k=1}^{\infty} \frac{1}{2k} W^{(\ell,k)} \frac{q_k^\bullet}{2}, \tag{4.18}$$

where $q_k^\bullet$ is given a factor $1/2$, as we either go up or down a value in the recursion and $q_k^\bullet$ had a factor 2, including both these options. Substituting now the pointed disk function, the cylinder function, and the face weight, it becomes

$$Q_\bullet^{(\ell)}(v) = \binom{2\ell}{\ell} R^\ell + \sum_{k=1}^{\infty} \frac{\ell}{\ell+k} \binom{2\ell}{\ell} \binom{2k}{k} R^{\ell+k} \sum_{p=0}^{\infty} \binom{p+k-1}{p} Q_\bullet^{(p)}(v). \tag{4.19}$$

This is valid for any vertex value v, but we will now restrict ourselves to the critical case $v = v_*$

4.2.1 Controlling number of level set jumps

If we find a function for $Q_\bullet^{(\ell)}(v_*)$, it has to satisfy this recursion relation. It would be even better to extract a closed solution from this equation. However, this is not so easy. We can introduce a new generating variable for controlling the change in vertex labels when crossing a level set. For this, we want to take into account that if (eventually) the vertex lies on a gasket, the value is either x or $x+1$ for $x \in 2\mathbb{Z}$. Without changing the probability distribution, we can take these two values as one. We do this by defining a variable for the vertex value

$$\lambda := \left\lfloor \frac{\text{label of marked vertex}}{2} \right\rfloor. \tag{4.20}$$

We can define a new generating function with this new generating variable like

$$Q_\bullet^{(\ell)}(v_*, \theta) := \sum_{\substack{\text{pointed labelled} \\ \text{quadrangulations } \mathfrak{q} \\ \text{of perimeter } \ell}} v_*^{|V(\mathfrak{q})|}\, e^{i\theta\lambda}, \tag{4.21}$$

which has the additional advantage that we can easily find the characteristic function for the random label λ via

$$\mathbb{E}[e^{i\theta\lambda}] = \frac{\sum_{\mathfrak{q}} v_*^{|V(\mathfrak{q})|}\, e^{i\theta\lambda}}{\sum_{\mathfrak{q}} v_*^{|V(\mathfrak{q})|}} = \frac{Q_\bullet^{(\ell)}(v_*, \theta)}{Q_\bullet^{(\ell)}(v_*, \theta = 0)}. \tag{4.22}$$

Additionally, we introduce the following variables, which are similar to those of the O(n) loop model [12, 13, 14, 16],

$$\theta = \pi b, \qquad n = 2\cos(\theta), \tag{4.23}$$

which are related via

$$\frac{n}{2} = \cos(\pi b), \qquad b = \frac{1}{\pi}\arccos\left(\frac{n}{2}\right). \tag{4.24}$$

The recurrence relation now becomes

$$Q_\bullet^{(\ell)}(v_*, \theta) = \binom{2\ell}{\ell} R^\ell + \frac{1}{2}\left(e^{i\theta} + e^{-i\theta}\right) \sum_{k=1}^{\infty} \frac{\ell}{\ell + k} \binom{2\ell}{\ell} \binom{2k}{k} R^{\ell+k} \sum_{p=0}^{\infty} \binom{p+k-1}{p} Q_\bullet^{(p)}(v_*, \theta). \tag{4.25}$$

Here, $e^{i\theta}$ indicates every time of going up a value, so from a $(x, x+1)$-gasket to a $(x+2, x+3)$-gasket, and $e^{-i\theta}$ indicates going down a value, so from $(x, x+1)$-gasket to a $(x-2, x-1)$-gasket (for $x \in 2\mathbb{Z}$). Substituting n, we get

$$Q_\bullet^{(\ell)}(v_*, \theta) = \binom{2\ell}{\ell} R^\ell + \frac{n}{2} \sum_{k=1}^{\infty} \frac{\ell}{\ell + k} \binom{2\ell}{\ell} \binom{2k}{k} R^{\ell+k} \sum_{p=0}^{\infty} \binom{p+k-1}{p} Q_\bullet^{(p)}(v_*, \theta). \tag{4.26}$$

Which in short notation is

$$Q_\bullet^{(\ell)} = W_\bullet^{(2\ell)} + \frac{n}{2} \sum_{k=1}^{\infty} \frac{1}{2k} W^{(\ell,k)} q_k^\bullet, \tag{4.27}$$

However, now solving this to get a closed solution is very hard and will probably yield a difficult expression. The generating function with a generating variable for the boundary length 2ℓ

$$Q_\bullet(x) = \sum_{\ell=0}^{\infty} x^{-\ell-1} Q_\bullet^{(\ell)}(v_*, \theta) \tag{4.28}$$

usually yields a simpler expression, for which we can use a transfer theorem to analyze the asymptotic behavior of $Q_\bullet^{(\ell)}(v_*, \theta)$ as $\ell \to \infty$. In the recurrence relation, we can multiply both sides by $x^{-\ell-1}$ and sum over all ℓ to get

$$Q_\bullet(x) = \sum_{\ell=0}^{\infty} x^{-\ell-1} \binom{2\ell}{\ell} R^\ell + \frac{n}{2} \sum_{\ell=0}^{\infty} x^{-\ell-1} \sum_{k=1}^{\infty} \frac{\ell}{\ell+k} \binom{2\ell}{\ell} \binom{2k}{k} R^{\ell+k} \sum_{p=0}^{\infty} \binom{p+k-1}{p} Q_\bullet^{(p)}(v_*, \theta). \tag{4.29}$$

We know that $R(v_*) = 1/8$ and we take x to be positive. This gives

$$Q_\bullet(x) = \frac{1}{\sqrt{x\left(x - \frac{1}{2}\right)}} + \frac{n}{2} \sum_{\ell=0}^{\infty} x^{-\ell-1} \sum_{k=1}^{\infty} \frac{\ell}{\ell+k} \binom{2\ell}{\ell} \binom{2k}{k} \left(\frac{1}{8}\right)^{\ell+k} \sum_{p=0}^{\infty} \binom{p+k-1}{p} Q_\bullet^{(p)}(v_*, \theta). \tag{4.30}$$

4.3 Solution for $Q_\bullet(x)$

Extracting a closed solution from (4.30) is rather difficult. So instead we take a different approach. In (4.18) we had the term

$$\frac{1}{2k} W^{(\ell,k)}, \tag{4.31}$$

which is the generating function of rooted maps of perimeter 2ℓ and a marked unrooted face of degree $2k$. We will define this as

$$W_k^{(\ell)} := \frac{1}{2k} W^{(\ell,k)} = \frac{1}{2} \frac{\ell}{\ell+k} \binom{2\ell}{\ell} \binom{2k}{k} R^{\ell+k}. \tag{4.32}$$

This can also be written as

$$W_k^{(\ell)} = \frac{1}{2} \int_0^R \frac{dr}{r}\, \ell \binom{2\ell}{\ell} r^\ell \binom{2k}{k} r^k \tag{4.33}$$

Since

$$\sum_{\ell=0}^{\infty} \binom{2\ell}{\ell} r^\ell z^{-\ell-1} = \frac{1}{\sqrt{z(z-4r)}} \qquad \text{and} \qquad \sum_{\ell=0}^{\infty} \ell \binom{2\ell}{\ell} r^\ell z^{-\ell-1} = r \frac{\partial}{\partial r} \frac{1}{\sqrt{z(z-4r)}}, \tag{4.34}$$

we find that

$$W(x,z) = \sum_{\ell=0}^{\infty} x^{-\ell-1} \sum_{k=0}^{\infty} z^{-k-1} W_k^{(\ell)} = \frac{1}{2} \int_0^R dr \frac{1}{\sqrt{z(z-4r)}} \frac{\partial}{\partial r} \frac{1}{\sqrt{x(x-4r)}}, \tag{4.35}$$

which can be integrated to get

$$\frac{z-4R}{2(z-x)\sqrt{x(x-4R)}\sqrt{z(z-4R)}} + \frac{1}{2} \frac{1}{x(x-z)}. \tag{4.36}$$

Introducing now the notation

$$f(x+i0) = \lim_{\epsilon \searrow 0} f(x+i\epsilon), \tag{4.37}$$

we get that for $x \in [0, 4R]$,

$$\sqrt{(x+i0)(x+i0-4R)} = -\sqrt{(x-i0)(x-i0-4R)}. \tag{4.38}$$

Therefore,

$$W(x+i0,z) + W(x-i0,z) = \frac{1}{x(x-z)}, \qquad \text{for } x \in [0,4R]. \tag{4.39}$$

As a reminder, the recursion relation in shorthand notation (4.27) with our new notation is now

$$Q_\bullet^{(\ell)} = W_\bullet^{(2\ell)} + \frac{n}{2} \sum_{k=1}^{\infty} W_k^{(\ell)} q_k^\bullet. \tag{4.40}$$

Multiplying by $x^{-\ell-1}$ and summing over all $\ell \geq 0$ yields

$$Q_\bullet(x) = W_\bullet(x) + \frac{1}{2\pi i} \frac{n}{2} \oint dz\, W(x,z)\, z\, q_\bullet(x) \tag{4.41}$$

$$= \frac{1}{\sqrt{x(x-4R)}} + \frac{1}{2\pi i} \oint dz\, W(x,z)\, n\, z\, Q_\bullet(1-x), \tag{4.42}$$

as $q_\bullet(x) = 2Q_\bullet(x)$. The term $W_\bullet(x)$ satisfies

$$W_\bullet(x+i0) + W_\bullet(x-i0) = 0. \tag{4.43}$$

So, for $x \in [0, 4R]$, we get that

$$Q_\bullet(x+i0) + Q_\bullet(x-i0) = \frac{1}{2\pi i} \oint dz\, \frac{1}{x(x-z)} nz Q_\bullet(1-x), \tag{4.44}$$

and by Cauchy's integral formula (and taking v critical, such that $R(v_*) = 1/8$), this becomes

$$Q_\bullet(x+i0) + Q_\bullet(x-i0) + nQ_\bullet(1-x) = 0, \qquad \text{for } x \in [0, 1/2]. \tag{4.45}$$

To obtain a solution for $Q_\bullet(x)$ from this equation, we can consult the solving strategy in [13] and follow the steps in Sections 3.2 and 3.3. Additionally, from [12, 13], we know that if we find a function for $Q_\bullet(x)$, it is a unique solution if 1) it has the right boundary conditions and 2) it satisfies equation (4.45). The starting point in the solving strategy is the equation

$$W_{\text{hom}}(x+i0) + W_{\text{hom}}(x+i0) - ns'(x) W_{\text{hom}}(s(x)) = 0, \qquad x \in [\gamma_-, \gamma_+]. \tag{4.46}$$

For us, $W_{\text{hom}}(x)$ represents $Q_\bullet(x)$ and the branch cut is $[0, 1/2]$. Here, $s(x)$ is defined by

$$s(x) = \frac{1-ahx}{ah + (1-a^2)h^2 x}. \tag{4.47}$$

If we now take $a = 1$ and $h = 0$, we get

$$s(x) = 1 - x, \tag{4.48}$$

such that we obtain (4.45) and hence

$$\gamma_- = 0, \quad \gamma_+ = \frac{1}{2}. \tag{4.49}$$

The solution is then given by

$$Q_\bullet(x(v)) = \frac{\omega(v)}{x'(v)}, \tag{4.50}$$

where

$$\omega(v) = \sum_{k\geq 0} a_k \left(\zeta^{(k)}(v - v_\infty) - \zeta^{(k)}(-v - v_\infty)\right). \tag{4.51}$$

This is thus a linear combination of $\zeta(v)$ and its derivatives, where $zeta(v)$ is given by

$$\zeta(v) = \cosh(bv)\coth(v) - \sinh(bv), \tag{4.52}$$

with

$$\pi b = \arccos\left(\frac{n}{2}\right). \tag{4.53}$$

The coefficients a_k are to be found via the boundary conditions later. We also have that

$$x(v) = (\gamma_+ - s(\gamma_-))\frac{\cosh(v) - 1}{\cosh(v) - \cosh(v_\infty)} + s(\gamma_-). \tag{4.54}$$

Here, $\cosh(v_\infty)$ is determined by $x(i\pi) = \gamma_-$, which gives $\cosh(v_\infty) = 0$, implying that $v_\infty = i\pi/2$. Filling in what we know, we get

$$x(v) = -\frac{1}{2}\left(\frac{\cosh(v) - 1}{\cosh(v)}\right) + 1 = \frac{1}{2}\left(\frac{1}{\cosh(v)} + 1\right). \tag{4.55}$$

We now invert $x(v)$ to get

$$v(x) = \operatorname{arccosh}\left(\frac{1}{2x - 1}\right). \tag{4.56}$$

For determining the coefficients a_k, we use Mathematica and expand $\omega(v)/x'(v)$ around $x \to \infty$ up to the third derivative[4]. We now want $Q_\bullet(x) = 1/x + \mathcal{O}(1/x^2)$ as $x \to \infty$. To get this, we can see that all coefficients other than a_0 have to be zero, and a_0 is chosen as such that we get the desired $1/x$. Plugging this in and so solving for $Q_\bullet(x)$, we obtain

$$Q_\bullet(x) = \frac{\sinh\left((1-b)\operatorname{arccosh}\left(\frac{1}{2x-1}\right)\right)}{x\sqrt{\frac{1}{x} - 1}\cos\frac{\pi b}{2}}. \tag{4.57}$$

Rewriting this in non-hyperbolic sinusoidal functions, this becomes

$$Q_\bullet(x) = \frac{\sin\left((1-b)\arccos\left(\frac{1}{2x-1}\right)\right)}{x\sqrt{1 - \frac{1}{x}}\cos\left(\frac{\pi b}{2}\right)} \tag{4.58}$$

Finally, the function must be symmetric in b, and we know that $\frac{n}{2} = \cos(\pi b)$, which is also symmetric in b. Therefore, we change b into $|b|$, giving us our final expression

[4]We could have taken higher order derivatives into account, but we see that only the linear term is nonzero

$$Q_\bullet(x) = \frac{\sin\left((1-|b|)\arccos\left(\frac{1}{2x-1}\right)\right)}{x\sqrt{1-\frac{1}{x}}\cos\left(\frac{\pi b}{2}\right)}. \tag{4.59}$$

By construction, $Q_\bullet(x)$ satisfies equation (4.45) and can be checked in Mathematica to have a branch cut on $[0, 1/2]$ (see Figure 4.3). For the uniqueness of $Q_\bullet(x)$, we additionally check if it has the right boundary conditions for $x \to \infty$ and $x \searrow 1/2$.

Firstly, we know that $Q(x) = \frac{Q^{(0)}}{x} + \mathcal{O}(\frac{1}{x^2}) = \frac{v}{x} + \mathcal{O}(\frac{1}{x^2})$, as $x \to \infty$, and that $Q_\bullet(x) = \frac{\partial}{\partial v}Q(x)$. Therefore, we should have that $Q_\bullet(x) = \frac{1}{x} + \mathcal{O}(\frac{1}{x^2})$, as $x \to \infty$ (which was actually already used in the construction).

Secondly, from [13] we know that as $x \searrow \gamma_+$ (so $x \searrow \frac{1}{2}$), $Q_\bullet(x)$ should behave as $Q_\bullet(x) \sim \frac{1}{(x-\frac{1}{2})^{1-|b|}}$ In short, these two come down to the following,

- as $x \to \infty$, $Q_\bullet(x) \sim \frac{1}{x}$;
- as $x \searrow \frac{1}{2}$, $Q_\bullet(x) \sim \frac{1}{(x-\frac{1}{2})^{1-|b|}}$

These conditions are confirmed with Mathematica, which means our solution for $Q_\bullet(x)$ is unique. We can perform two additional sanity checks to ensure (4.59) is the correct function.

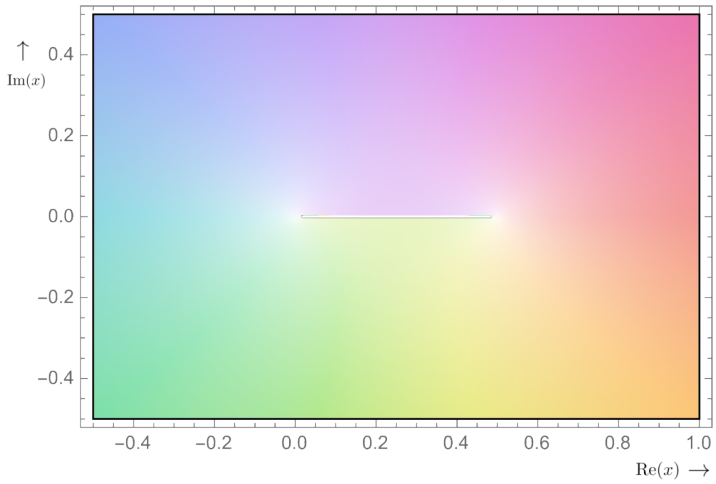

Figure 4.3: The branch cut of $Q_\bullet(x)$, which is [0,1/2].

If $b = 0$ ($n = 2$), we can use inverse trigonometric identities to rewrite $Q_\bullet(x)$ to $Q_\bullet(x) = \frac{1}{x-\frac{1}{2}}$ Moreover, this yields $Q^{(\ell)}(v_*) = 2^{-\ell}$, which we can check with the recursion relation (4.26). As a reminder, this relation was

$$Q_\bullet^{(\ell)}(v_*,\theta) = \binom{2\ell}{\ell}\left(\frac{1}{8}\right)^\ell + \frac{n}{2}\sum_{k=1}^{\infty}\frac{\ell}{\ell+k}\binom{2\ell}{\ell}\binom{2k}{k}\left(\frac{1}{8}\right)^{\ell+k}\sum_{p=0}^{\infty}\binom{p+k-1}{p}Q_\bullet^{(p)}(v_*,\theta). \tag{4.60}$$

We will look at the right-hand side and check if it gives back $2^{-\ell}$ for $n = 2$. We first note that

$$\sum_{p=0}^{\infty}\binom{p+k-1}{p}2^{-p} = 2^k. \tag{4.61}$$

Therefore, we have

$$\binom{2\ell}{\ell}\left(\frac{1}{8}\right)^{\ell}+\binom{2\ell}{\ell}\left(\frac{1}{8}\right)^{\ell}\sum_{k=1}^{\infty}\frac{\ell}{\ell+k}\binom{2k}{k}\left(\frac{1}{8}\right)^{k}2^{k}. \tag{4.62}$$

We then evaluate the sum with WolframAlpha, giving

$$\sum_{k=1}^{\infty}\frac{\ell}{\ell+k}\binom{2k}{k}\left(\frac{1}{8}\right)^{k}2^{k}=\frac{\sqrt{\pi}\,\Gamma(\ell+1)}{\Gamma(\ell+\frac{1}{2})}-1, \tag{4.63}$$

by which we are left with

$$\frac{\sqrt{\pi}\,\Gamma(\ell+1)}{\Gamma(\ell+\frac{1}{2})}\binom{2\ell}{\ell}\left(\frac{1}{8}\right)^{\ell}, \tag{4.64}$$

which is exactly $2^{-\ell}$.

If now $b=\frac{1}{2}$ ($n=0$), we see in (4.30) that we should get $Q_\bullet(x)=\frac{1}{\sqrt{x(x-\frac{1}{2})}}$. By substituting $b=\frac{1}{2}$ in (4.59) (for $x>0$ and $R>0$), we exactly obtain this result. Therefore, we conclude that we have found the correct and unique solution for $Q_\bullet(x)$.

4.4 Statistical distribution of the label value

The statistical distribution can be obtained by finding the characteristic function $\varphi_\lambda(\theta)$ of the label value λ for $\ell\to\infty$ and then checking which known distribution shares that characteristic function. We start with the characteristic function

$$\varphi_\lambda(\theta)=\mathbb{E}^{(\ell)}[e^{i\theta\lambda}]=\frac{\sum_{\mathfrak{q}}v_*^{|V(\mathfrak{q})|}e^{i\theta\lambda}}{\sum_{\mathfrak{q}}v_*^{|V(\mathfrak{q})|}}=\frac{Q_\bullet^{(\ell)}(v_*,\theta)}{Q_\bullet^{(\ell)}(v_*,0)}. \tag{4.65}$$

When $\theta=0$, we have $n=2$, for which we found that $Q^{(\ell)}(v_*,0)=2^{-\ell}$. However, we do not have an exact expression for arbitrary θ. As we are interested in the asymptotic behavior at $\ell\to\infty$, we will use a transfer theorem from [17], which we will use apply to $Q_\bullet(x)$.

Theorem 4.2 (Transfer theorem [17])**.** *Assume that*

$$f(z)\sim(1-z)^{-\alpha},\qquad \text{as } z\to 1,$$

with $\alpha\notin\mathbb{Z}_{\le 0}$. The coefficients of $f(z)$ then satisfy

$$[z^n]f(z)\sim\frac{n^{\alpha-1}}{\Gamma(\alpha)},\qquad \text{as } n\to\infty.$$

Continuing with (4.65) and leaving the limit for a moment,

$$\frac{Q_\bullet^{(\ell)}(v_*,\theta)}{Q_\bullet^{(\ell)}(v_*,0)}=\frac{[x^{-\ell-1}]Q_\bullet(x)}{Q_\bullet^{(\ell)}(v_*)}=2^{\ell}[x^{-\ell-1}]\frac{\sin\left((1-|b|)\arccos\left(\frac{1}{2x-1}\right)\right)}{x\sqrt{1-\frac{1}{x}}\cos\left(\frac{\pi b}{2}\right)}. \tag{4.66}$$

We will look at $x\to\frac{1}{2}$, where we had that

$$Q_\bullet(x)\sim\frac{1}{\cos(\frac{\pi b}{2})}\frac{1}{\left(x-\frac{1}{2}\right)^{1-|b|}}. \tag{4.67}$$

Hence, we want to solve

$$2^{\ell}[x^{-\ell-1}]\frac{1}{\cos(\frac{\pi b}{2})}\frac{1}{\left(x-\frac{1}{2}\right)^{1-|b|}}. \tag{4.68}$$

To match the requisites of the transfer theorem, we take $x=\frac{1}{2z}$, such that we get

$$\frac{2^{\ell}}{\cos(\frac{\pi b}{2})}[(2z)^{\ell+1}]\frac{1}{\left(\frac{1}{2z}-\frac{1}{2}\right)^{1-|b|}}, \tag{4.69}$$

$$=\frac{2^{\ell}}{\cos(\frac{\pi b}{2})}[z^{\ell}]\frac{2^{-\ell-1}}{z}\frac{1}{\left(\frac{1}{2}\right)^{1-|b|}(1-z)^{1-|b|}\,z^{|b|-1}}, \tag{4.70}$$

but $z\to 1$, so

$$=\frac{1}{\left(\frac{1}{2}\right)^{-|b|}\cos(\frac{\pi b}{2})}[z^{\ell}]\frac{1}{(1-z)^{1-|b|}}. \tag{4.71}$$

Applying now the transfer theorem, we then end up with

$$\mathbb{E}^{(\ell)}[e^{i\theta\lambda}]=\frac{Q_{\bullet}^{(\ell)}(v_*,\theta)}{Q_{\bullet}^{(\ell)}(v_*,0)}\sim\frac{1}{\left(\frac{1}{2}\right)^{-|b|}\cos(\frac{\pi b}{2})}\frac{\ell^{-|b|}}{\Gamma(1-|b|)}=C(|b|)\ell^{-|b|},\qquad\text{as }\ell\to\infty. \tag{4.72}$$

where

$$C(|b|)=\frac{1}{\left(\frac{1}{2}\right)^{-|b|}\cos(\frac{\pi b}{2})\Gamma(1-|b|)}. \tag{4.73}$$

This diverges, however. To solve this, we introduce now the renormalized label

$$\Lambda:=\frac{\lambda}{\log(\ell)}. \tag{4.74}$$

The characteristic equation for Λ is

$$\varphi_{\Lambda}(\alpha)=\lim_{\ell\to\infty}\mathbb{E}^{(\ell)}[e^{i\alpha\Lambda}]=\lim_{\ell\to\infty}\mathbb{E}^{(\ell)}[e^{i\frac{\alpha}{\log(\ell)}\lambda}] \tag{4.75}$$

$$=\lim_{\ell\to\infty}\mathbb{E}^{(\ell)}[e^{i\theta\lambda}] \tag{4.76}$$

where we have taken that

$$\theta=\frac{\alpha}{\log(\ell)},\quad b=\frac{\theta}{\pi}=\frac{\alpha}{\pi\log(\ell)}. \tag{4.77}$$

As $\ell\to\infty$, we have $\theta\to 0$ and thus $b\to 0$, such that

$$\lim_{\ell\to\infty}\mathbb{E}^{(\ell)}[e^{i\theta\lambda}]=\lim_{\ell\to\infty}C(b)\ell^{-|b|} \tag{4.78}$$

$$=\lim_{\ell\to\infty}C\left(\frac{|\alpha|}{\pi\log(\ell)}\right)\ell^{-\frac{|\alpha|}{\pi\log(\ell)}} \tag{4.79}$$

$$=C(0)e^{-\frac{|\alpha|}{\pi}} \tag{4.80}$$

$$=e^{-\frac{|\alpha|}{\pi}}. \tag{4.81}$$

Therefore, we have

$$\varphi_{\Lambda}(\alpha)=e^{-\frac{|\alpha|}{\pi}}. \tag{4.82}$$

We also know from probability theory that the Cauchy distribution Φ has probability distribution

$$\frac{1}{\pi}\frac{\mathrm{dx}}{x^2+1}. \tag{4.83}$$

Hence, the characteristic function of a Cauchy distributed variable X is

$$\varphi_X(t) = \mathbb{E}[e^{iXt}] = \frac{1}{\pi}\int_{-\infty}^{\infty}\frac{e^{iXt}}{x^2+1}dx = e^{-|t|}. \tag{4.84}$$

By Lévy's continuity theorem [17], we can thus conclude that for $\ell \to \infty$, Λ converges in distribution to the Cauchy distribution Φ. Consequently, the value of the labels λ converges in distribution to the Cauchy distribution and scales with $\log(\ell)$,

$$\lambda \xrightarrow{(d)} \frac{\Phi}{\log(\ell)}. \tag{4.85}$$

5 Conclusion and discussion

In this thesis, we looked at 2D Quantum Gravity coupled to a scalar field, where we discretized the geometries and represented this with integer-labeled maps. We imposed the condition on the scalar field so that it cannot deviate very much via the colorful labeling of the maps. As the combinatorics of Boltzmann maps are well understood, we made a connection between these and our model. The universality class of this model is seen to be non-generic critical with critical exponent $\alpha = 3/2$, meaning the surfaces are fractal. With the method of gasket decomposition, we set up a recurrence relation, confirming its usefulness. With the solving strategy from the work of Borot, Bouttier and Guitter [12], we could establish the unique function for $Q_\bullet(x)$. As our main result, we then showed with the help of a transfer theorem that the values of the colorful quadrangulations are distributed along the Cauchy distribution and scale with $\log(\ell)$. This means that when we couple a massless scalar field to 2D Quantum Gravity, the values of this scalar field are Cauchy distributed and scale with $\log(\ell)$, yielding a notion of correlation. In contrast, for a scalar field on a discretized square lattice with the same gradient restriction, the scalar field value also scales logarithmically with the boundary length but is expected to be normally distributed [18]. This is an interesting change induced by the coupling to 2D Quantum Gravity. We have also seen that adding matter changed the geometry of our problem as the critical exponent in the absence of matter ($\mathrm{LQG}_{\gamma=\sqrt{8/3}}$) is $\alpha = 2$ [6], while coupled to a massless scalar field ($\mathrm{LQG}_{\gamma=2}$) we found it to be $\alpha = 3/2$. Furthermore, we can interpret the scaling of the values as the influence matter has on each other, which we expect. This all was previously seen via the generating functions of these labeled quadrangulations, established in [15]. This thesis, however, aimed to do this enumeration via the method of gasket decomposition, which has proven useful and is arguably easier than the work of Bousquet-Mélou and Price [15].

We did all of the above for a critical vertex value v_*, greatly simplifying the problem. If not for this, the solutions would have been elliptic functions, adding a whole new layer to the problem. For us, $v = v_*$ was enough, as it allowed us to find the critical exponent and the statistical distribution. However, it might be insightful to analyze this model leaving v a variable. In the future, it might also be interesting to couple more interesting fields to 2D Quantum gravity and find out how matter influences other matter here. However, with more 'interesting' comes more complicated. Therefore, finding ways to couple more complex fields to Quantum Gravity and determining what LQG universality class it is in might be insightful. The model of colorful quadrangulations is proven to be in bijection with so-called rigid quadrangulations, and it could be interesting to explore this to better our understanding of the combinatorics of this model. Furthermore, in [14], for the O(n) loop model, a relation was observed between the number of loops surrounding a marked vertex and the total winding angle of a simple random walk, with some initial conditions. Perhaps, a relation to a similar random can be found for these colorful quadrangulations.

Acknowledgements

I would like to thank Timothy Budd for his excellent guidance during my bachelor's thesis. During the last half year, we held weekly discussions, which were always very insightful and instructive and inspired me time and time again to continue working on the problem. I also want to thank my roommates, Gijs and Luuk, for filling my breaks with chats, laughter, and the occasional game of darts. Last but not least, thanks to Anastasia for her love and support and for proofreading this thesis.

References

[1] Michael E. Peskin and Daniel V. Schroeder. *Introduction to quantum field theory.* CRC Press LLC, 2019.

[2] Sean M. Carroll. *Spacetime and geometry: An introduction to general relativity.* Cambridge University Press, 2023.

[3] John A. Wheeler and Kenneth W. Ford. *Geons, black holes, and quantum foam: A life in physics.* Norton, 2000.

[4] M. Anyon and J. Dunning-Davies. A fresh look at some questions surrounding black holes. June 2008.

[5] Thomas Hartman. Lectures on quantum gravity and black holes. Lecture notes, 2015.

[6] Timothy Budd. Lessons from the mathematics of two-dimensional euclidean quantum gravity. December 2022.

[7] Jan Groenendijk. Tree bijections in two-dimensional quantum gravity. Bachelor Thesis, Radboud University, 2021.

[8] Pjotr Koster. Universality classes of 2d hyperbolic riemannian manifolds. Bachelor Thesis, 2022.

[9] Jian Ding, Julien Dubedat, and Ewain Gwynne. Introduction to the liouville quantum gravity metric. September 2021.

[10] Timo Weigand. Quantum field theory i + ii.

[11] Timothy Budd. Random geometry in the path integral approach to quantum gravity. Exercise sheet, May 2023.

[12] Gaëtan Borot, Jérémie Bouttier, and Bertrand Duplantier. Nesting statistics in the o(n) loop model on random planar maps. May 2016.

[13] G. Borot, J. Bouttier, and E. Guitter. More on the o(n) model on random maps via nested loops: loops with bending energy. *J. Phys. A: Math. Theor. 45 (2012) 275206*, February 2012.

[14] Timothy Budd. The peeling process on random planar maps coupled to an o(n) loop model (with an appendix by linxiao chen). September 2018.

[15] Mireille Bousquet-Mélou and Andrew Elvey Price. The generating function of planar eulerian orientations. *J. Combin. Theory Ser. A 2020*, March 2018.

[16] G. Borot, J. Bouttier, and E. Guitter. A recursive approach to the o(n) model on random maps via nested loops. *J. Phys. A: Math. Theor. 45 (2012) 045002*, June 2011.

[17] Robert Sedgewick Philippe Flajolet. *Analytic Combinatorics.* 2009.

[18] Hugo Duminil-Copin, Matan Harel, Benoit Laslier, Aran Raoufi, and Gourab Ray. Logarithmic variance for the height function of square-ice. *Communications in Mathematical Physics*, 396(2):867–902, September 2022.